ARTICLE IN PRESS

Alexandria Engineering Journal (2017) xxx, xxx–xxx

HOSTED BY

ELSEVIER

Alexandria University

Alexandria Engineering Journal

www.elsevier.com/locate/aej
www.sciencedirect.com

ORIGINAL ARTICLE

A comparative study of chemically reacting 2D flow of Casson and Maxwell fluids

M. Sathish Kumar [a], N. Sandeep [a,*], B. Rushi Kumar [a], S. Saleem [b,c]

[a] Department of Mathematics, VIT University, Vellore 632014, India
[b] Department of Sciences and Humanities, National University of Computer & Emerging Sciences, Pakistan
[c] Department of Mathematics, Statistics and Physics, Qatar University, Doha 2713, Qatar

Received 6 October 2016; revised 27 April 2017; accepted 7 May 2017

KEYWORDS

MHD;
Casson and Maxwell fluids;
Stretching sheet;
Thermophoresis;
Brownian motion

Abstract Theoretical investigation is performed to discuss the heat and mass transfer behavior of chemically reacting magnetohydrodynamic Casson and Maxwell fluids past a stretching sheet with Brownian moment and thermophoresis effects with internal heat source/sink. Runge-Kutta based shooting procedure is employed to yield the solutions of the problem. Effects of the pertinent parameters on velocity, thermal and concentration boundary layers are analyzed through graphical illustrations. Also computed the reduced Nusselt and Sherwood numbers and presented through tables. It is found that the boundary layers of temperature and concentration fields are non-uniform for Casson and Maxwell fluids. Thermal and concentration fields of Maxwell fluid is highly influenced by the pertinent parameters when compared with the Casson fluid.

1. Introduction

The study of magnetohydrodynamic flows over a stretching surface has mesmerized the many researchers because of their important applications in manufacturing and industrial processing. Especially, the study of MHD boundary layer flows has numerous applications in the chemical engineering and metallurgy processing, such that thinning of copper wire, wire drawing, astrophysical plasmas annealing and delineation of space, etc. The concept of nanofluid by involving the nano meter sized particles was first explained by Choi [1]. Many investigations are made to study the Maxwell fluid flow past a stretching sheet under various conditions. Non-Newtonian fluid is classified into tree types, such as rate, differential and integral type fluid. In these, the fluid consider a rate type is called a Maxwell fluid. The Maxwell fluid was first proposed by Maxwell in 1867. Recently, Sandeep and Sulochana [2] explained heat transfer bearing the Maxwell fluid flow past a stretching sheet by considering the space and temperature dependent source/sink. The study of magnetohydrodynamic flows over a stretched channel has charmed by the authors [3–7]. Afify [8] discussed the numerical study of MHD convection flow and heat transfer past a stretching surface by considering the chemical reaction. Many researchers investigated the flow and mass transfer of UCM (upper convected Maxwell fluid) flow with various regimes. Sadeghy et al. [9] studied the MHD flow of upper convected Maxwell fluid past vertical plate. The influence uniform magnetic field on Casson fluid

* Corresponding author.
E-mail address: dr.nsrh@gmail.com (N. Sandeep).
Peer review under responsibility of Faculty of Engineering, Alexandria University.

http://dx.doi.org/10.1016/j.aej.2017.05.010
1110-0168

Nomenclature

a	positive constant (S^{-1})
B_0	constant magnetic field ($kg/(s^2\,A)$)
Bi	Biot number
C	nanoparticle concentration (kg/m^3)
C_∞, C_f	free stream and surface particle concentrations (kg/m^3)
C_f	coefficient of skin friction
C_p	specific heat ($J/(kg\,K)$)
D_B	coefficient of Brownian diffusion (m^2/s)
D_T	coefficient of thermophoretic diffusion (m^2/s)
f	similarity variable
k	thermal conductivity of the fluid ($W/(m\,K)$)
Le	Lewis number
M	magnetic field parameter
Nb	Brownian moment parameter
Nt	thermophoresis parameter
Nu_x	reduced Nusselt number
Sh_x	reduced Sherwood number
Pr	Prandtl number
T	fluid temperature
T_∞, T_f	free stream and surface fluid temperatures (K)
u, v	flow component along the x and y direction (m/s)
x, y	Cartesian coordinates (m)
k_0	is the relaxation time
Q_0	heat generation/absorption coefficient
k_1	rate of chemical reaction

Greek symbols

α	thermal diffusivity (m^2/s)
γ	chemical reaction parameter
δ	heat source/sink parameter
η	similarity variable
θ	dimensionless temperature
λ	elastic parameter
μ	dynamic viscosity of the fluid (kg/m s)
v	kinematic viscosity capacity of the nanoparticle material (m^2/s)
ρ_f	fluid density (kg/m^3)
$(\rho C_p)_f$	heat capacity of the fluid ($J/(m^3\,K)$)
$(\rho C_p)_s$	specific heat capacity of the particles ($J/(m^3\,K)$)
τ	nanoparticle to base fluid heat capacity ratio
φ	dimensionless nanoparticle concentration
ψ	dimensionless stream function

Subscripts

f	surface condition
∞	free stream condition

flow past an exponentially located sheet was studied by Nadeem et al. [10].

Casson fluid was first introduced by Casson in 1959. Casson fluid is a shear thinning fluid which is alleged to have an limitless viscosity at zero rate, if yield stress under which no flows occurs. If viscosity is zero at an infinite rate, then the shear stress is less than the yield stress then it act as a solid. Casson fluid examples are as follows, tomato sauce, jelly, soup, honey and juices. Casson fluid contains human blood properties, because of its blood cells structure and the substance like fibrinogen, protein, rouleaux etc. The effect of MHD flow on Casson fluid past a stretching surface was investigated by Hayat et al. [11]. The researchers [12–14] studied the effect of MHD and porosity parameter on the flow past stretching surface. The heat transfer behavior of radiative Casson fluid flow past a stretching surface was analyzed by Pramanik [15]. He found that rising values of Casson parameter depreciate the flow field. Abolbashari et al. [16] studied the entropy generation of magnetohydrodynamic nanofluid flow over a permeable sheet. The study of heat transfer in nanofluid flow between parallel plates with Brownian moment by using DTM was analyzed by Sheikholeslami and Ganji [17]. Sheikholeslami et al. [18] studied the heat transfer of nanofluid with the variable magnetic field and found that rising values of Hartmann number depreciate the reduced Nusselt number.

By using entropy generation method (thermodynamic optimization or finite time thermodynamics), the nanofluid in a channel by considering the thermophoresis, Brownian motion and thermal radiation was investigated by Mahmoodi and Kandelousi [19]. Heidary et al. [20] illustrated the impact of magnetic field on nanofluid flow and heat transfer over a straight channel. In this study, they concluded that increasing values of Hartmann number enhances the heat transfer rate. Abolbashari et al. [21] analytically investigated the heat transfer of Casson nanofluid flow past a stretching sheet in the presence of velocity slip conditions by using Homotopy Analysis Method. Nanofluid flow between parallel plates by considering the various physical effects was studied by Sheikholeslami et al. [22] and concluded that rising the Brownian moment declines the rate of heat transfer.

Sandeep and Sulochana [23] discussed the buoyancy effects on magnetohydrodynamic flow past a shrinking surface and found that buoyancy forces regulate the flow field. The elasticity influence on MHD flow of Maxwell fluid over a stretched sheet with Brownian moment was studied by Nadeem et al. [24]. Very recently, the studies [25–29] reported on convective heat transfer in magnetohydrodynamic flows. The effects of Brownian motion and thermophoresis on MHD flow and heat transfer of Maxwell fluid over a stretching sheet was examined by Hayat et al. [32]. Abbasi and Shehzad [33] discussed the influence of Cattaneo-Christov heat flux on 3D MHD flow of Maxwell fluid over a bidirectioncal stretching surface with heat absorption/generation effect. Th MHD heat and mass transfer flow of Maxwell fluid over a linear stretching sheet in the presence of Brownian motion and thermophoresis effects was presented by Abbasi et al. [34].

In all the above investigations author's focused on analyzing the heat or heat and mass transfer characteristics of some MHD flows by considering one or two physical effects. But in this study, we discussed the flow, thermal and mass transport behavior of chemically reacting magnetohydrodynamic flow past a stretched sheet by considering the various physical effects namely, internal heat source/sink, variable heat source/sink, Brownian moment and thermophoresis effects. Numerical solutions are presented by making use of R-K based shooting method. Results are discussed with the help of graphs and tables.

Please cite this article in press as: M.S. Kumar et al., A comparative study of chemically reacting 2D flow of Casson and Maxwell fluids, Alexandria Eng. J. (2017), http://dx.doi.org/10.1016/j.aej.2017.05.010

2. Mathematical formulation

Consider a magnetohydrodynamic flow of Casson and Maxwell nanofluids over a stretching surface placed along x-axis and y-axis is perpendicular to it. A transverse magnetic field B_0 is functioned along flow direction as depicted in Fig. 1. We considered that the underlying part of the sheet is filled with hot fluid. Here $u_w = ax$, (a is a constant) is a stretched velocity of a sheet and T_f and C_w are the temperature and concentration of the fluid near the boundary. We assumed an internal heat source along with chemical reaction of first order. We also considered the cross diffusion effects with Brownian movement and thermophoresis. We ignored viscous dissipation and induced magnetic field effects. With the assumptions stated above, the governing equations in terms of similarity variable can be expressed [30,31]

$$\frac{\partial^2\psi}{\partial x\partial y} - \frac{\partial^2\psi}{\partial y\partial x} = 0, \tag{1}$$

$$\frac{\partial\psi}{\partial y}\frac{\partial^2\psi}{\partial x\partial y} - \frac{\partial\psi}{\partial x}\frac{\partial^2\psi}{\partial y^2} + k_0\left(\left(\frac{\partial\psi}{\partial y}\right)^2\frac{\partial^2\psi}{\partial x^2\partial y} + \left(\frac{\partial\psi}{\partial x}\right)^2\frac{\partial^3\psi}{\partial y^3} - 2\frac{\partial^2\psi}{\partial y\partial x}\frac{\partial^3\psi}{\partial x\partial y^2}\right) = v\left(1+\frac{1}{\beta}\right)\frac{\partial^3\psi}{\partial y^3} - \frac{\sigma B_0^2}{\rho_f}\left(\frac{\partial\psi}{\partial y} + k_0 v\frac{\partial^2\psi}{\partial y^2}\right), \tag{2}$$

$$\frac{\partial\psi}{\partial y}\frac{\partial T}{\partial x} - \frac{\partial\psi}{\partial x}\frac{\partial T}{\partial y} = \alpha\frac{\partial^2 T}{\partial y^2} + \tau\left(\frac{\partial C}{\partial y}\frac{\partial T}{\partial y} + \frac{D_T}{T_\infty}\left(\frac{\partial T}{\partial y}\right)^2\right) + \frac{Q_0}{\rho c_p}(T - T_\infty) + \frac{k u_w}{x v} \times \frac{1}{\rho c_p}(A^*(T_w - T_\infty) + B^*(T - T_\infty)), \tag{3}$$

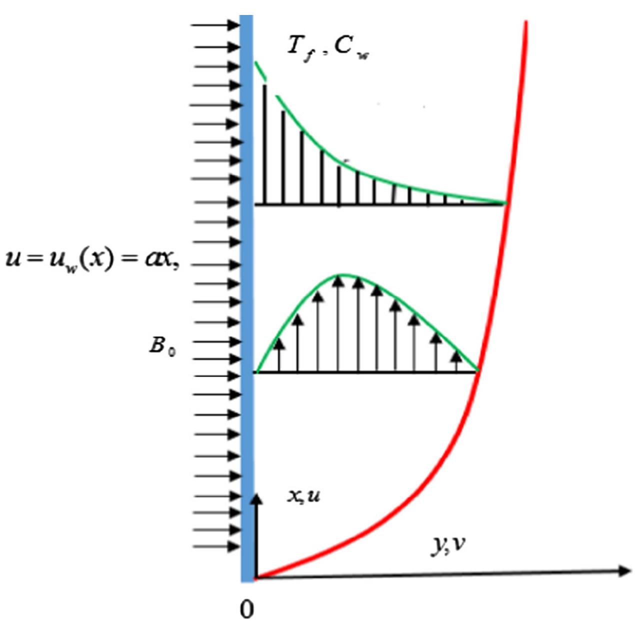

Figure 1 Physical model of the problem.

$$\frac{\partial\psi}{\partial y}\frac{\partial C}{\partial x} - \frac{\partial\psi}{\partial x}\frac{\partial C}{\partial y} = D_B\frac{\partial^2 C}{\partial y^2} + \frac{D_T}{T_\infty}\frac{\partial^2 T}{\partial y^2} - k_1(C - C_\infty), \tag{4}$$

with the conditions

$$u = ax = u_w,\quad v = 0,\quad -k\frac{\partial T}{(T_f - T)} = h_f\partial y,\quad C = C_w,\quad at\quad y = 0,$$
$$u(\infty) = 0,\quad T(\infty) = T_\infty,\quad C(\infty) = C_\infty, \tag{5}$$

The following non-dimensional variables are introduced:

$$\eta = (a/v)^{0.5}y,\quad \psi(x,y) = (av)^{0.5}xf(\eta),$$
$$T = (T_f - T_\infty)\theta(\eta) + T_\infty,\quad C = (C_w - C_\infty)\varphi(\eta) + C_\infty, \tag{6}$$

where $\psi(x,y)$ is the stream function pointed by

$$u = \frac{\partial\psi}{\partial y}\quad and\quad v = -\frac{\partial\psi}{\partial x}, \tag{7}$$

which automatically fulfil the continuity Eq. (1). In view of Eq. (6), the Eqs. (2)–(5) become

$$\left(1+\frac{1}{\beta}\right)\frac{\partial^3 f}{\partial\eta^3} - M\frac{\partial f}{\partial\eta} + f(1+\lambda M)\frac{\partial^2 f}{\partial\eta^2} - \lambda\left(\frac{\partial^3 f}{\partial\eta^3}f^2 - 2f\frac{\partial f}{\partial\eta}\frac{\partial^2 f}{\partial\eta^2}\right) - \left(\frac{\partial f}{\partial\eta}\right)^2 = 0, \tag{8}$$

$$\frac{\partial^2\theta}{\partial\eta^2} + Pr\left(f\frac{\partial\theta}{\partial\eta} + \delta\theta + Nb\frac{\partial\varphi}{\partial\eta}\frac{\partial\theta}{\partial\eta} + Nt\left(\frac{\partial\theta}{\partial\eta}\right)^2\right) + \delta\theta + A^*f' + B^*\theta = 0, \tag{9}$$

$$\frac{\partial^2\varphi}{\partial\eta^2} + Lef\frac{\partial\varphi}{\partial\eta} + \frac{Nt}{Nb}\frac{\partial^2\theta}{\partial\eta^2} - \gamma Le\varphi = 0, \tag{10}$$

With the boundary conditions being

$$F'(\eta) = 1,\quad f(\eta) = 0,\quad \varphi(\eta) = 1,\quad \theta'(\eta) = -Bi(1-\theta(\eta)),\quad at\quad \eta = 0,$$
$$f'(\infty) = 0,\quad \theta(\infty) = 0,\quad \varphi(\infty) = 0, \tag{11}$$

The non-dimensional parameters are given by

$$Pr = \frac{v}{\alpha},\quad Le = \frac{v}{D_B},\quad Bi = (h_f/k)\sqrt{v/a},\quad \lambda = ak_0,$$

$$\delta = Q_0/(\rho C_p a),\quad M = B_0\sqrt{\sigma/(\rho_f a)}$$

$$Nb = \frac{((\rho C)_p D_B(C_w - C_\infty))}{((\rho C)_f v)},\quad Nt = \frac{((\rho C)_p D_T(T_f - T_\infty))}{((\rho C)_f v T_\infty)},$$

It should be mentioned that $\gamma > 0$ and $\gamma < 0$ respectively represent the destructive and generative chemical reactions, while $\delta > 0$ and $\delta < 0$ corresponds to heat source and sink respectively.

The physical quantities of interest are the friction factor C_f, reduced Nusselt and Sherwood numbers Nu_x and Sh_x are given by

$$C_f = \frac{\tau_w}{\rho u_w^2},\quad Nu_x = \frac{\chi q_w}{k(T_f - T_\infty)},\quad Sh_x = \frac{\chi h_m}{D_B(C_w - C_\infty)} \tag{12}$$

where τ_w – shear stress, and q_w *and* h_m are the surface heat and mass flux, respectively:

Please cite this article in press as: M.S. Kumar et al., A comparative study of chemically reacting 2D flow of Casson and Maxwell fluids, Alexandria Eng. J. (2017), http://dx.doi.org/10.1016/j.aej.2017.05.010

$$\tau_w = \mu\left(1 + \frac{1}{\beta}\right)(1 + \lambda)\left(\frac{\partial u}{\partial y}\right)_{y=0}, \quad q_w = -k\left(\frac{\partial T}{\partial y}\right)_{y=0},$$
$$h_m = -D_B\left(\frac{\partial C}{\partial y}\right)_{y=0} \tag{13}$$

The dimensionless forms of skin friction, the local Nusselt number, and the local Sherwood number become

$$Re_x^{1/2} C_f = \left(1 + \frac{1}{\beta}\right)(1 + \lambda) f''(0), \quad \frac{Nu_x}{Re_x^{1/2}} = -\theta'(0),$$
$$\frac{Sh_x}{Re_x^{1/2}} = -\varphi'(0), \tag{14}$$

where $Re_x = xu_w/v$ local Reynolds number.

3. Solution procedure

The numerical solution of the governing system of coupled ODEs (8)–(10) under the boundary restrictions Eq. (11) is obtained with the assist of Runge–Kutta based shooting technique with step size as $\eta = 0.001$ and relative error as 10^{-6}. Set of nonlinear ordinary differential equations are of third order in f second order in θ and ϕ are first reduced into a system of simultaneous ordinary equations as shown below. In order to solve this system using Runge-Kutta with shooting method, one should require three more missed initial conditions. However, the values of $f'(\eta)$, $\theta(\eta)$ and $\phi(\eta)$ are known when $\eta \to \infty$. These end conditions are used to obtain the unknown initial conditions at $\eta = 0$ using shooting technique.

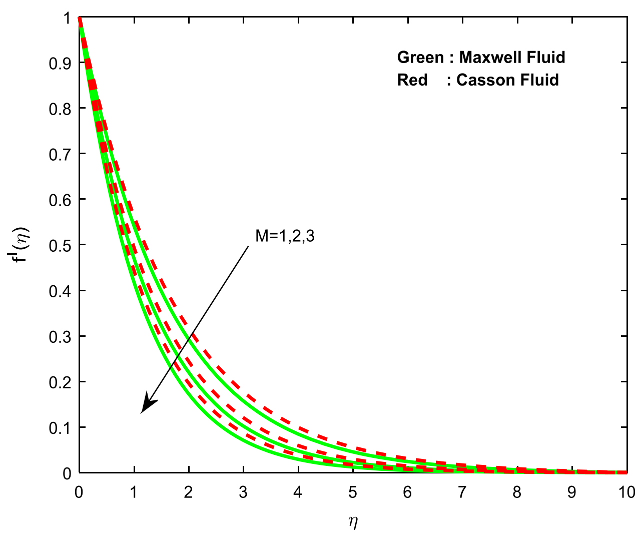

Figure 2 Variation $f'(\eta)$ with M.

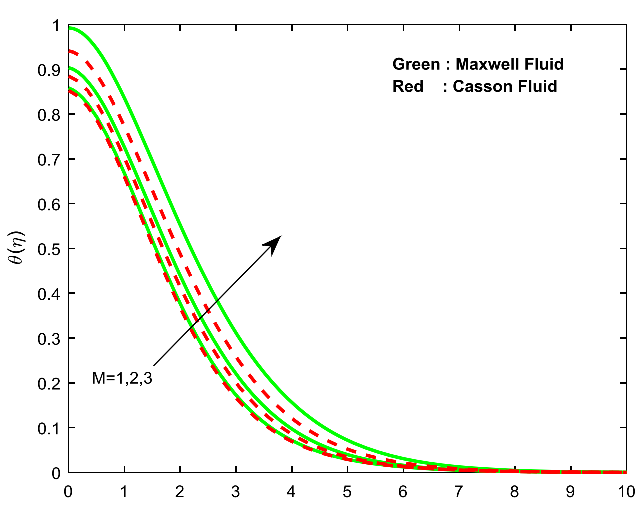

Figure 3 Variation $\theta(\eta)$ with M.

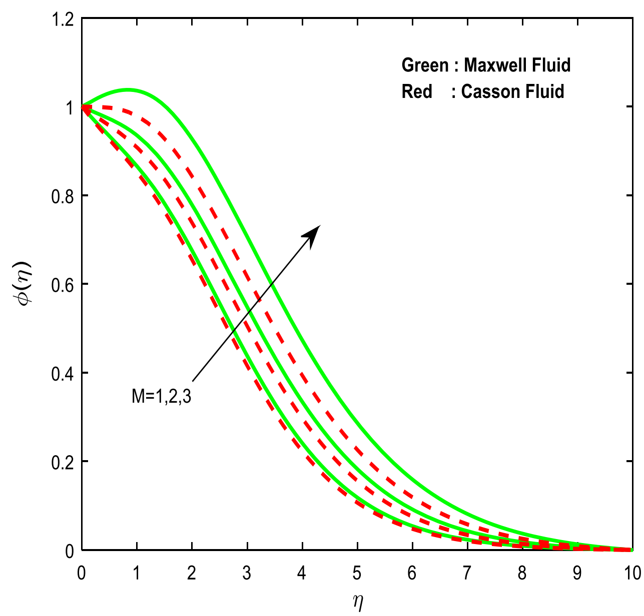

Figure 4 Variation $\phi(\eta)$ with M.

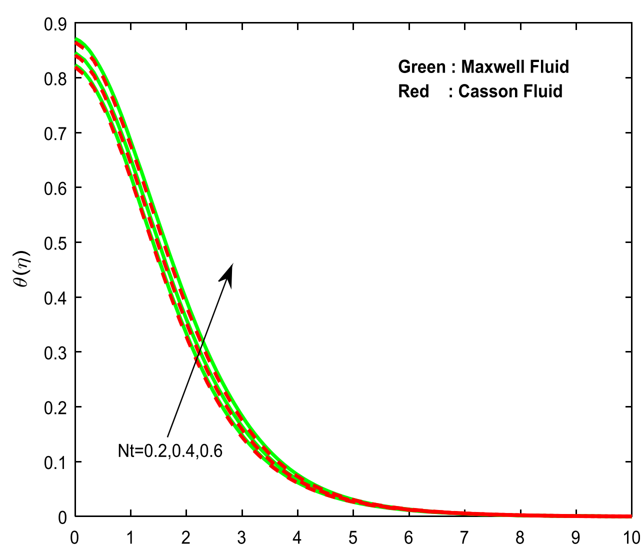

Figure 5 Variation $\theta(\eta)$ with Nt.

Please cite this article in press as: M.S. Kumar et al., A comparative study of chemically reacting 2D flow of Casson and Maxwell fluids, Alexandria Eng. J. (2017), http://dx.doi.org/10.1016/j.aej.2017.05.010

4. Results and discussion

The transformed Odes' (8)–(10) with the conditions Eq. (11) are solved numerically using R-K based shooting method. Results shows the effect of magnetic field parameter (M), chemical reaction parameters (γ), Lewis number (Le), Biot number (Bi), variable heat sources/sink parameter (A^*, B^*), Brownian movement parameter (Nb) and thermophoresis parameter (Nt) on the flow, thermal and concentration fields. In this study, we consider the pertinent parameters values as $\beta = 0.5, \lambda = 2, M = 1, Pr = 6, Bi = 0.3, Le = 0.6, Nb = Nt = 0.5, A^* = B^* = 0.2, \delta = 0.5, \gamma = 0.2$.

Figs. 2–4 depict the velocity, thermal and concentration fields for different values of the magnetic field parameter M. It is observed that both the thermal and concentration distributions displayed an increasing behavior for rising values of M. But the flow field $f'(\eta)$ reduces for enhancing the values of the magnetic field parameter. Physically, rising values of magnetic field parameter develops the negative strength to the flow. This negative strength is capable to depreciate the flow field and encourage the temperature field.

Increasing values of thermophoretic parameter enhances the thickness of both thermal and concentration as shown in Figs. 5 and 6. Generally, thermophoretic parameter improves

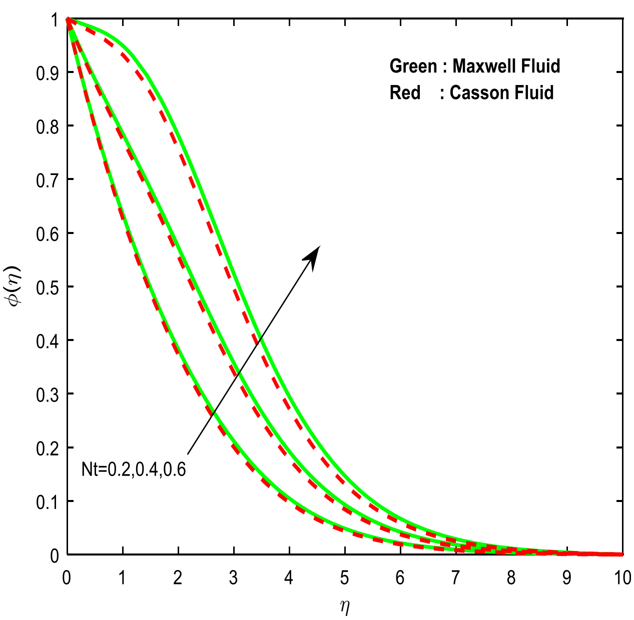

Figure 6 Variation $\phi(\eta)$ with Nt.

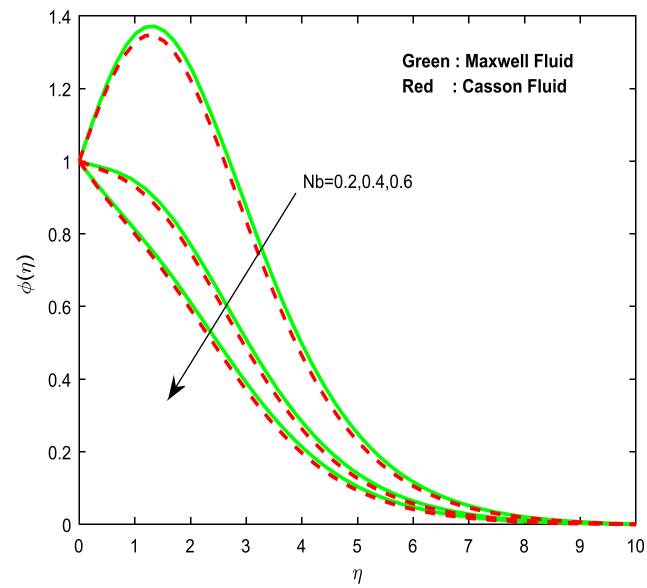

Figure 8 Variation $\phi(\eta)$ with Nb.

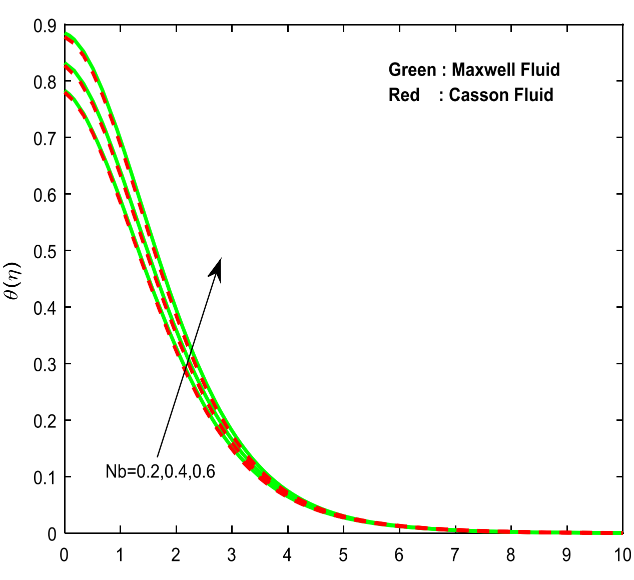

Figure 7 Variation $\theta(\eta)$ with Nb.

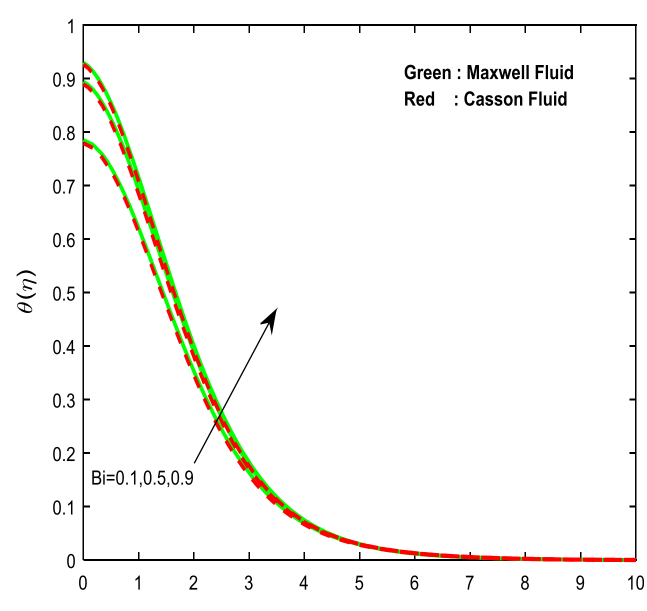

Figure 9 Variation $\theta(\eta)$ with Bi.

Please cite this article in press as: M.S. Kumar et al., A comparative study of chemically reacting 2D flow of Casson and Maxwell fluids, Alexandria Eng. J. (2017), http://dx.doi.org/10.1016/j.aej.2017.05.010

the thermal filed apart from the heat generated by the sheet. Figs. 7 and 8 show the influence of Nb on the thermal and concentration fields. We observed a rise in the temperature and a fall in the concentration for increasing values of Nb. This is due to the random motion of the particles and enhances the augmentation of the temperature profile.

Figs. 9 and 10 illustrate the influence of Biot number on the thermal and concentration fields. We observed that increasing the Biot number enhances the thermal and concentration fields. The impact of A^* on temperature and concentration distribution is shown in Figs. 11 and 12. It is clear that rising values of A^* increases both temperature and concentration distribution. Generally, positive values of the non-uniform heat source/sink parameter acts as heat generators.

Fig. 13 demonstrates the effect of γ on concentration profiles. It can be noticed that rise in γ depreciate the concentration profile. Fig. 14 displays the influence of the Lewis number on concentration profile. It is observed that rising values of Lewis number decreasing the concentration profile. Because of this mass transfer rate enhances as Lewis number increases.

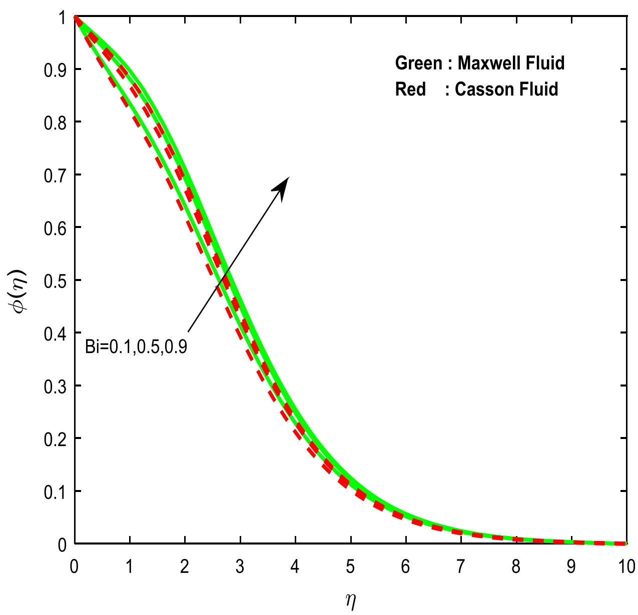

Figure 10 Variation $\phi(\eta)$ with Bi.

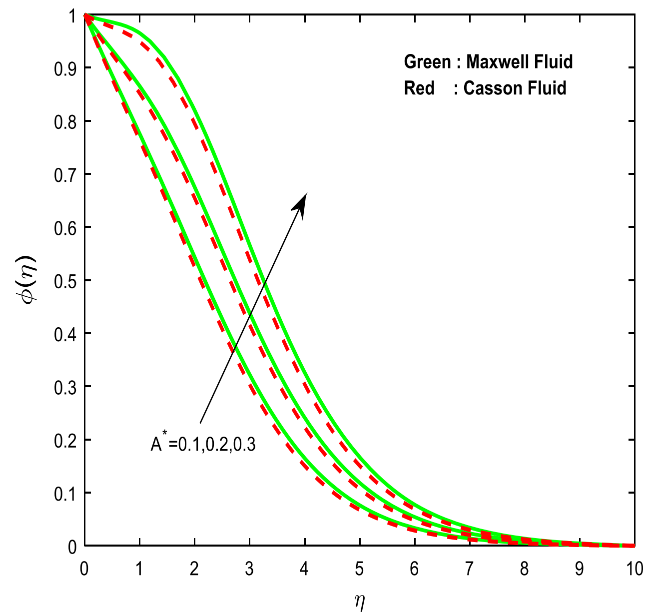

Figure 12 Variation $\phi(\eta)$ with A^*.

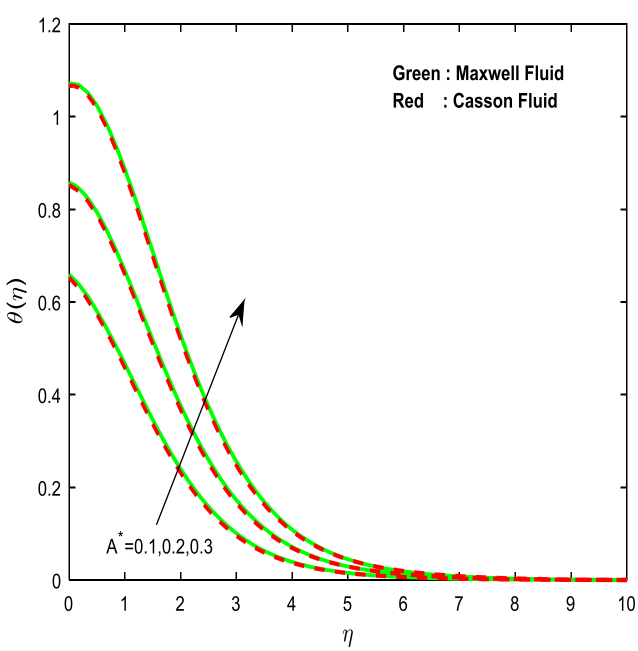

Figure 11 Variation $\theta(\eta)$ with A^*.

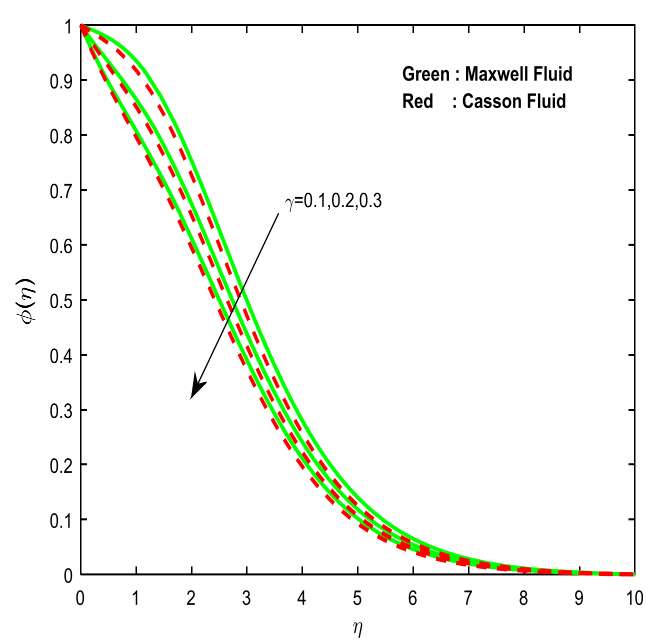

Figure 13 Variation $\phi(\eta)$ with γ.

Please cite this article in press as: M.S. Kumar et al., A comparative study of chemically reacting 2D flow of Casson and Maxwell fluids, Alexandria Eng. J. (2017), http://dx.doi.org/10.1016/j.aej.2017.05.010

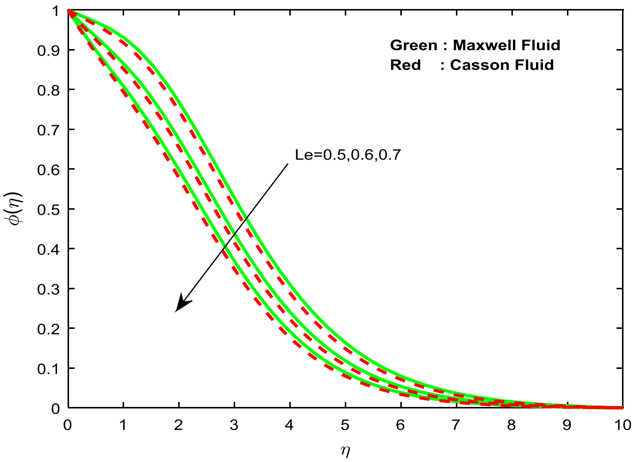

Figure 14 Variation $\phi(\eta)$ with Le.

Tables 1 and 2 display the variation in local Nusselt and Sherwood numbers at various pertinent parameters for Maxwell and Casson fluids. It is obvious that rising values of thermophoresis parameter, Brownian motion parameter, magnetic field parameter and non-uniform heat sources/sink parameter depreciate the heat transfer rate. But for higher values of Biot number enhance the heat transfer rate. But Brownian motion, chemical reaction parameter and Lewis number have tendency to enhance the mass transfer rate. The validation of the results is displayed in Table 3.

5. Conclusions

Theoretical investigation is performed to discuss the heat and mass transfer behavior of chemically reacting magnetohydrodynamic Casson and Maxwell fluids past a stretching sheet with Brownian moment and thermophoresis effects with internal heat source/sink. Runge-Kutta based shooting procedure is employed to yield the solutions of the problem. Effects of the pertinent parameters on velocity, thermal and concentration boundary layers are analyzed through graphical illustrations. Findings of the present study are as follows:

- Increasing values of magnetic field depreciate the heat and mass transfer rate.
- Biot number have tendency to encourage the heat transfer rate.
- Rising values of the thermophoresis improves the concentration and thermal fields.
- Mass transfer rate is high for boosting values of the chemical reaction parameter.
- Thermal and concentration fields of Maxwell fluid is highly influenced by applied magnetic field when compared with the Casson fluid.

Table 1 Variations in local Nusselt and Sherwood numbers for Maxwell fluid.

M	Nt	Nb	Bi	A^*	γ	Le	$-\theta'(0)$	$-\phi'(0)$
1							0.042583	0.147250
2							0.028972	0.061533
3							0.002323	−0.064223
	0.2						0.053023	0.430740
	0.4						0.046314	0.246611
	0.6						0.038532	0.042002
		0.2					0.065048	−0.450556
		0.4					0.050350	0.048594
		0.6					0.034534	0.212318
			0.1				0.021473	0.192399
			0.5				0.052892	0.124744
			0.9				0.062976	0.102394
				0.1			0.102152	0.238562
				0.2			0.042583	0.147250
				0.3			−0.021657	0.044713
					0.1		0.044601	0.041941
					0.2		0.042583	0.147250
					0.3		0.041019	0.237857
						0.5	0.046053	0.065954
						0.6	0.042583	0.147250
						0.7	0.039950	0.221811

Table 2 Variations in local Nusselt and Sherwood numbers for Casson fluid.

M	Nt	Nb	Bi	A^*	γ	Le	$-\theta'(0)$	$-\phi'(0)$
1							0.044299	0.164045
2							0.034654	0.094806
3							0.017759	0.006734
	0.2						0.054080	0.439508
	0.4						0.047779	0.260220
	0.6						0.040545	0.062669
		0.2					0.065944	−0.424800
		0.4					0.051774	0.066774
		0.6					0.036563	0.228267
			0.1				0.022087	0.208593
			0.5				0.055333	0.141470
			0.9				0.066253	0.118811
				0.1			0.104149	0.253652
				0.2			0.044299	0.164045
				0.3			−0.019934	0.064379
					0.1		0.046143	0.062589
					0.2		0.044299	0.164045
					0.3		0.042849	0.251980
						0.5	0.047616	0.082447
						0.6	0.044299	0.164045
						0.7	0.041777	0.238678

Table 3 Validation of the present results for various values of Nt when $M=\lambda=\gamma=\delta=0, Bi=0.1, Pr=Le=10$ *and* $Nb=0.1$.

Nt	Makinde and Aziz [35]		Present results	
	$-\theta'(0)$	$-\varphi'(0)$	$-\theta'(0)$	$-\varphi'(0)$
0.1	0.0929	2.2774	0.09291	2.27744
0.2	0.0927	2.2490	0.09270	2.24905
0.3	0.0925	2.2228	0.09252	2.22282
0.4	0.0923	2.1992	0.09231	2.19921
0.5	0.0921	2.1783	0.09210	2.17830

Please cite this article in press as: M.S. Kumar et al., A comparative study of chemically reacting 2D flow of Casson and Maxwell fluids, Alexandria Eng. J. (2017), http://dx.doi.org/10.1016/j.aej.2017.05.010

References

[1] S.U.S. Choi, Enhancing thermal conductivity of fluids with nano particles, Proc ASME Int. Mech. Eng. Congr. Exposition 66 (1995) 99–105.

[2] N. Sandeep, C. Sulochana, Momentum and heat transfer behaviour of Jeffrey, Maxwell and Oldroyd-B nanofluids past a stretching surface with non-uniform heat source/sink, Ain Shams Eng. J. (2016), http://dx.doi.org/10.1016/j.asej.2016.02.008 (in press).

[3] T.R. Mahapatra, A.S. Gupta, Magnetohydrodynamic stagnation-point flow towards a stretching sheet, Acta Mech. 152 (2001) 191–196.

[4] T.R. Mahapatra, A.S. Gupta, Heat transfer in stagnation point flow towards stretching sheet, Heat Mass Transf. 389 (2002) 517–521.

[5] A. Ishak, R. Nazar, I. Pop, Mixed convection boundary layer in the stagnation point flow towards a stretching vertical sheet, Meccanica 41 (2006) 509–518.

[6] A. Ishak, K. Jafar, R. Nazar, I. Pop, MHD stagnation point flows towards a stretching sheet, Physica A 388 (2009) 3377–3383.

[7] T.R. Mahapatra, S.K. Nandy, A.S. Gupta, Magnetohydrodynamic stagnation point flow of a power-law fluid towards a stretching sheet, Int. J. Non-Linear Mech. 44 (2009) 124–129.

[8] A.A. Afify, MHD free convective flow and mass transfer over a stretching sheet with chemical reaction, Heat Mass Transf. 40 (2004) 495–500.

[9] K. Sadeghy, A.H. Najafi, M. Saffaripour, Sakiadis flow of an upper-convected Maxwell fluid, Int. J. Non-Linear Mech. 40 (2005) 1220–1228.

[10] S. Nadeem, R. Ul Haq, C. Lee, MHD flow of a Casson fluid over an exponentially Shrinking sheet, Sci. Iran. 19 (6) (2012) 1550–1553.

[11] T. Hayat, S.A. Shehzad, A. Alsaedi, Soret and Dufor effects on Magneto hydrodynamics flow of Casson fluid, Appl. Math. Mech. 33 (10) (2012) 1301–1312.

[12] S. Nadeem, Rizwan Ul Haq, N.S. Akbar, Z.H. Khan, MHD three-dimensional Casson fluid flow past a porous linearly stretching sheet, Alexandria Eng. J. 52 (2013) 577–582.

[13] N.S. Akbar, S. Nadeem, Rizwan Ul Haq, Z.H. Khan, Radiation effects on MHD stagnation point flow of nanofluid towards a stretching surface with convective boundary condition, Chin. J. Aeronaut. 26 (6) (2013) 1389–1397.

[14] S. Nadeem, Rizwan Ul Haq, Z.H. Khan, Heat transfer analysis of water-based nanofluid over an exponentially stretching sheet, Alex. Eng. J. 53 (2014) 219–224.

[15] S. Pramanik, Casson fluid flow and heat transfer past an exponentially porous stretching sheet in presence of thermal radiation, Ain Shams Eng. J. 5 (2014) 205–212.

[16] M.H. Abolbashari, Navid Freidoonimehr, Foad Nazari, M.M. Rasidi, Entropy analysis for an unsteady MHD flow past a stretching permeable surface in nano-fluid, Powder Tech. 267 (2014) 256–267.

[17] M. Sheikholeslami, D.D. Ganji, Nanofluid flow and heat transfer between parallel plates considering Brownian motion using DTM, Comput. Methods Appl. Mech. Eng. 283 (2015) 651–663.

[18] M. Sheikholeslami, M.M. Rashidi, D.D. Ganji, Effects of non-uniform magnetic field on forced convection heat transfer of Fe_3O_4] -water nanofluid, Comput. Methods Appl. Mech. Eng. 294 (2015) 299–312.

[19] M. Mahmoodi, Sh. Kandelousi, Effects of thermoresis and Brownian motion on nanofluid heat transfer and entropy generation, J. Mol. Liq. 211 (2015) 15–24.

[20] H. Heidary, R. Hosseini, M. Pirmohammadi, M.J. Kermani, Numerical study of magnetic field effect on nanofluid forced convection in a channel, J. Magn. Magn. Mater. 374 (2015) 11–17.

[21] M.H. Abolbashari, N. Freidoonimehr, F. Nazari, M.M. Rashidi, Analytical modelling of entropy generation for Casson nano-fluid flow induced by a stretching surface, Adv. Powder Tech. 26 (2015) 542–552.

[22] M. Sheikholeslami, M.M. Rashidi, D.M. Al Sadd, F. Firouzi, H.B. Rokni, G. Domairry, Steady nanofluid flow between parallel plates considering thermophoresis and Brownian effects, J. King Saud Univ.-Sci. 28 (4) (2015) 380–389.

[23] N. Sandeep, C. Sulochana, Dual solutions for unsteady mixed convection flow of MHD micropolar fluid over a stretching/shrinking sheet with non-uniform heat source/sink, Eng. Sci. Technol. Int. J. 18 (2015) 738–745.

[24] S. Nadeem, Rizwan Ul Haq, Z.H. Khan, Numerical study of MHD boundary layer flow of Maxwell fluid past a stretching sheet in the presence of nanoparticles, J. Taiwan Inst. Chem. Eng. 45 (2014) 121–126.

[25] G. Kumaran, N. Sandeep, Thermophoresis and Brownian moment effects on parabolic flow of MHD Casson and Williamson fluids with cross diffusion, J. Mol. Liq. 233 (2017) 262–269.

[26] N. Sandeep, Ram Prakash Sharma, M. Ferdows, Enhanced heat transfer in unsteady magnetohydrodynamic nanofluid flow embedded with aluminum alloy nanoparticles, J. Mol. Liq. 234 (2017) 437–443.

[27] M. Jayachandra Babu, N. Sandeep, UCM flow across a melting surface in the presence of double stratification and cross-diffusion effects, J. Mol. Liq. 232 (2017) 27–35.

[28] A. Khalid, I. Khan, A. Khan, S. Shafie, Unsteady MHD free convection flow of Casson fluid past over an oscillating vertical plate embedded in a porous medium, Eng. Sci. Technol. Int. J. 18 (2015) 309–317.

[29] N. Sandeep, Effect of aligned magnetic field on liquid thin film flow of magnetic-nanofluid embedded with graphene nanoparticles, Adv. Powder Technol. 28 (2017) 865–875.

[30] J. Buongiorno, Convective transport in nanofluids, ASME J. Heat Transf. 128 (2006) 240–250.

[31] S.S. Motsa, T. Hayat, O.M. Aldossary, MHD flow of upper-convected Maxwell fluid over porous stretching sheet using Successive Taylor serious linearization method, Appl. Math. Mech. – Engl. Ed. 33 (2012) 975–990.

[32] T. Hayat, T. Muhammad, S.A. Shehzad, A. Alsaedi, Three dimensional rotating flow of Maxwell nanofluid, J. Mol. Liq. 229 (2017) 495–500.

[33] F.M. Abbasi, S.A. Shehzad, Heat transfer analysis for three-dimensional flow of Maxwell fluid with temperature dependent thermal conductivity: application of Cattaneo-Christov heat flux model, J. Mol. Liq. 220 (2016) 848–854.

[34] F.M. Abbasi, S.A. Shehzad, T. Hayat, B. Ahmad, Doubly stratified mixed convection flow of Maxwell nanofluid with heat generation/absorption, J. Magn. Magn. Mater. 404 (2016) 159–165.

[35] O.D. Makinde, A. Aziz, Boundary layer flow of a nanofluid past a stretching sheet with a convective boundary condition, Int. J. Therm. Sci. 50 (2011) 1326–1332.

Please cite this article in press as: M.S. Kumar et al., A comparative study of chemically reacting 2D flow of Casson and Maxwell fluids, Alexandria Eng. J. (2017), http://dx.doi.org/10.1016/j.aej.2017.05.010